JOURNAL OF SOLID STATE CHEMISTRY 83, 78–90 (1989)

Dimorphism, Phase Transitions, and Transport Properties in $LiZr_2(PO_4)_3$

F. SUDREAU, D. PETIT, AND J. P. BOILOT

Groupe de Chimie du Solide, Laboratoire de Physique de la Matière Condensée, Ecole Polytechnique, 91128 Palaiseau Cédex, France

Received February 6, 1989

We report the structure, the phase transitions, and the transport properties of two different phases of $LiZr_2(PO_4)_3$ materials prepared by the sol/gel technique. The phases have been characterized by X-ray powder diffractometry, thermal analysis, ac conductivity, and NMR (^{31}P and ^{7}Li). A high-temperature phase, prepared at 1200°C, shows a NASICON-type structure and a monoclinic → rhombohedral first order transition at about 40°C. This transformation is associated with the sharp appearance of a lithium motion leading to high conducting properties above the phase transition $\sigma = 1.2.10^{-2}$ $(\Omega\ cm)^{-1}$ at 300°C. A low-temperature phase, prepared at 900°C, exhibits the β-$Fe_2(SO_4)_3$-type structure and a monoclinic → orthorhombic transformation at 300°C. A local lithium motion progressively takes place between RT and 120°C and a conducting state is observed at 300°C ($\sigma = 5.10^{-4}$ $(\Omega\ cm)^{-1}$). In diphasic samples prepared between 900 and 1200°C, both resistivity and activation energy progressively increase with the low–high temperature phase ratio.

Introduction

NASICON (Na super ionic conductor) compounds exhibit exceptionally high ionic conductivities allowing them to perform like the best alkaline superionic conductors, such as β'' alumina. Typical NASICON materials are produced from the solid solution $Na_{1+x}Zr_2P_{3-x}Si_xO_{12}$ formed between sodium–zirconium phosphate ($x = 0$) and silicate ($x = 3$) with a pronounced maximum of conductivity for composition around $x = 2$ ($Na_3Zr_2PSi_2O_{12}$) (*1*, *2*).

The purpose of this paper is to study the NASICON analog lithium phosphate $LiZr_2(PO_4)_3$. In fact, previous results concerning the structure and conductivity of this compound appeared somewhat confused.

First, $LiZr_2(PO_4)_3$ powders and ceramics have been prepared by conventional processing using solid state reactions. Following this procedure, preparation of rhombohedral (Sljukic *et al.* (*3*)) and of slightly distorted (Taylor *et al.* (*4*)) NASICON-type phases has been reported. Moreover, Subramamian *et al.* (*5*) claimed that after firing at 1100°C, the X-ray pattern of $LiZr_2(PO_4)_3$ was highly distorted and a triclinic cell was possibly present. The ionic conductivity seems to be very low: $<10^{-9}$ $(\Omega\ cm)^{-1}$ at RT and 2.10^{-5} $(\Omega\ cm)^{-1}$ at 300°C.

Second, as typical NASICON compositions (*6*), $LiZr_2(PO_4)_3$ ceramics have been prepared from highly reactive powders based on calcined gels. Sol–gel routes lead to submicronic powders which sinter with

0022-4596/89 $3.00

short thermal treatment, a few hundred degrees lower than typical oxide powders. Following the sol–gel method:

(i) Perthuis and Colomban (*7*) and Barj *et al.* (*8*) reported the preparation of a NASICON-type phase with the usual crossover from a monoclinic to a rhombohedral symmetry at 50°C. This leads to high conducting properties above 300°C: 2.10^{-3} $(\Omega\ cm)^{-1}$ at 350°C for a sample fired at 1050°C.

(ii) Petit *et al.* (*9*) observed two phase transitions: at a temperature (25–60°C) depending on the firing temperature of the sample, the usual monoclinic → rhombohedral transition was observed; a second phase transition was noted at about 280°C leading to a long-range lithium motion (*10*). At 350°C, the conductivity is 5.10^{-4} $(\Omega\ cm)^{-1}$ for a sample fired at 1100°C.

(iii) Finally, Casciola *et al.* (*11*) prepared $LiZr_2(PO_4)_3$ by a wet chemical technique, starting from aqueous solutions of $ZrOCl_2$, H_3PO_4, and LiOH. The material fired at 900°C exhibits a monoclinic → orthorhombic change at 300°C which is obviously not consistent with the NASICON-type structure. The conductivity of sintered pellets at 900°C is 7.10^{-4} $(\Omega\ cm)^{-1}$ at 300°C.

All these previous studies suggest the existence of two structural forms for $LiZr_2(PO_4)_3$: a high-temperature NASICON-type phase prepared above 1200°C and a low-temperature phase prepared at 900°C. We describe sol–gel preparation, structure, phase transitions, and transport properties of these two forms which have been characterized by X-ray powder diffractometry, thermal analysis, ac conductivity, and NMR (^{31}P and ^{7}Li). Diphasic samples prepared between 900 and 1200°C were also investigated.

Experimental

$LiZr_2(PO_4)_3$ powders were prepared by the sol–gel method described previously by Perthuis and Colomban (*7*). An alcoholic solution containing zirconium propoxide $Zr(O^nC_3H_7)_4$, held under vigorous stirring, was hydrolyzed by an aqueous mixture of $NH_4H_2PO_4$ and $LiNO_3$ heated at 80°C. $Zr(O^nC_3H_7)_4$ was supplied by Alfa Ventron and other reagents by Merck. The effective Zr composition of the alkoxide was controlled by weighing the zirconium oxide obtained after hydrolysis and heating at 1200°C. The gel was then placed in a vacuum drying oven at 60°C for 10 hr. The amorphous xerogel powder was composed of small spherical aggregates 200 nm in size. Crystallization of xerogels occured gradually in the 600–800°C temperature range.

Ceramic processing consisted of pressing in the xerogel powder at 400 MPa and sintering at different temperatures (900–1300°C) for 3–6 hr in an atmosphere with lithium oxide source ($LiZr_2(PO_4)_3$ powder) to reduce the stoichiometry deviation. Moreover the composition was controlled and regulated by chemical analysis of Li, Zr, and P elements performed by the Service Central d'Analyse du CNRS. The densification factor progressively increased from 85 to 95% with increasing sintering temperature from 900 to 1250°C.

Powder X-ray diffraction (XRD) and differential scanning calorimetry (DSC4 Perkin–Elmer) were used to characterize selected pellets and powders.

Measurements of ac conductivity were achieved according to the temperature (RT–400°C) on sintered disks (10 mm in diameter and 2 mm thick) by means of an HP 4192 A impedance analyzer (input impedance of 10 MΩ) with frequencies ranging from 10 Hz to 13 MHz. The electrodes were made from a flux containing platinum lake deposited on the polished surfaces (thermal treatment at 800°C for 3 hr). ^{31}P and ^{7}Li NMR spectra were recorded on a Brucker MSL 360 spectrometer. For MAS spectra, samples were packed in alumina rotors and

spun at roughly 4.5 kHz in a magic-angle spinning probe from Doty Scientific.

Results

1. High-Temperature Phase

Structure and phase transition. XRD patterns from $LiZr_2(PO_4)_3$ powders heated at 1200°C show the usual reflections corresponding to the NASICON-type structure (Fig. 1). However, at room temperature a slight splitting of the rhombohedral reflections takes place due to the well-known monoclinic deformation (*12*). Above 50°C, this deformation disappears and the lattice is rhombohedral ($R\bar{3}c$ space group) with the hexagonal parameters $a = 8.85$ Å and $c = 22.24$ Å and the volume by unit formula $V/Z = 251.4$ Å^3.

The structure of NASICON compounds (*1*) can be broken down into fundamental groups of two zirconium octahedra (O) separated by three phosphorus tetrahedra (T) with which they share corner oxygens. These basic structural units O_2T_3, parallel to the c hexagonal axis, join by additional corner sharing, which results in a three-dimensional quasi-cubic framework (Fig. 2a). In the rhombohedral structure, lithium ions occupy octahedral polyhedra at each intersection of three conduction channels (*9*).

The monoclinic → rhombohedral transformation is always accompanied by a significant thermal effect. All the specimens heated in the 1200–1300°C temperature range exhibit a single reproducible anomaly with hysteresis on the DSC curves (Fig. 3a), corresponding to a first order transition. Neither transition enthalpy (about 3 kJ mol^{-1}) nor peak position (maximum at 40°C and onset at 30°C) change drastically with the length of the thermal treatment. However, it should be noted that some samples show a broad peak during the first scan (Fig. 3b) and a normal behavior during following scans.

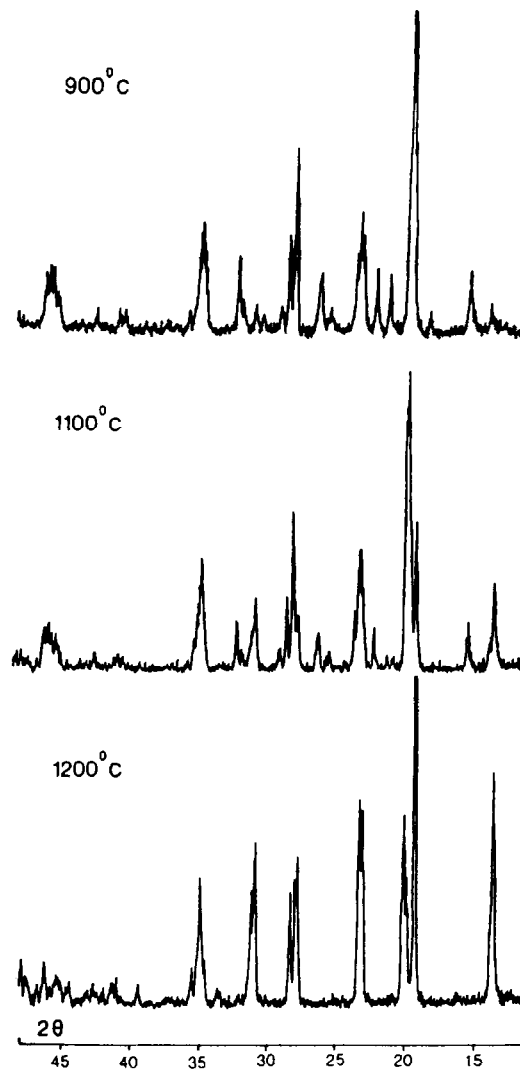

FIG. 1. X-ray diffraction patterns for $LiZr_2(PO_4)_3$ powders heated for 6 hr at different temperatures. The patterns correspond to the pure low-temperature phase at 900°C, the pure high-temperature phase at 1200°C, and the mixture of the two phases at 1100°C.

Below the phase transition, ^{31}P MAS NMR spectra present three peaks (Fig. 4a) corresponding to three crystallographically distinct positions for the phosphorus atoms. For the monoclinic NASICON-type structure, the systematic extinctions ($h + k = 2n$, $h0l = 2n$) are consistent with the two

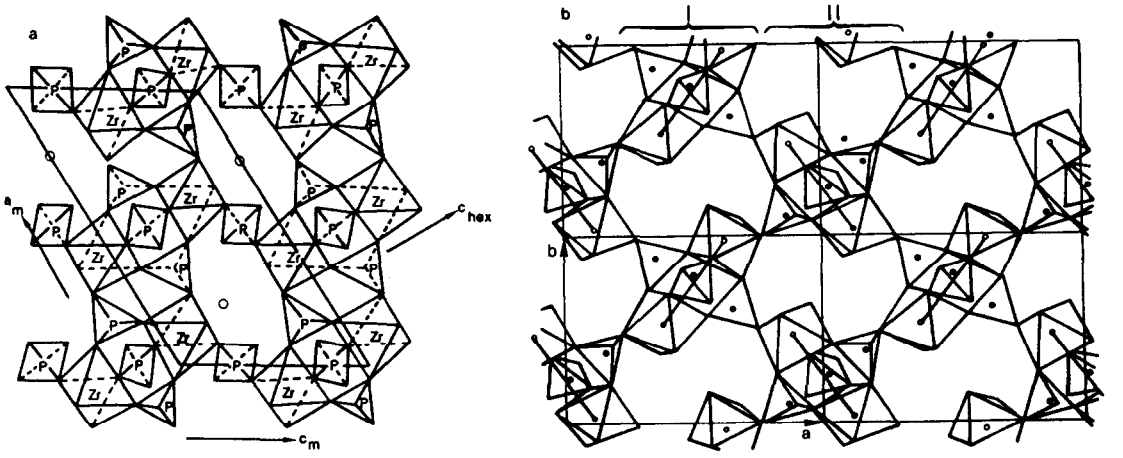

FIG. 2. Structure of the two phases of $LiZr_2(PO_4)_3$. (a) High-temperature phase: projection of half the unit cell along the a_r-axis of the rhombohedral NASICON-type structure (Ref. (*1*)). (b) Low-temperature phase: projection in the (001) plane of the β-$Fe_2(SO_4)_3$ monoclinic-type structure (Ref. (*18*)).

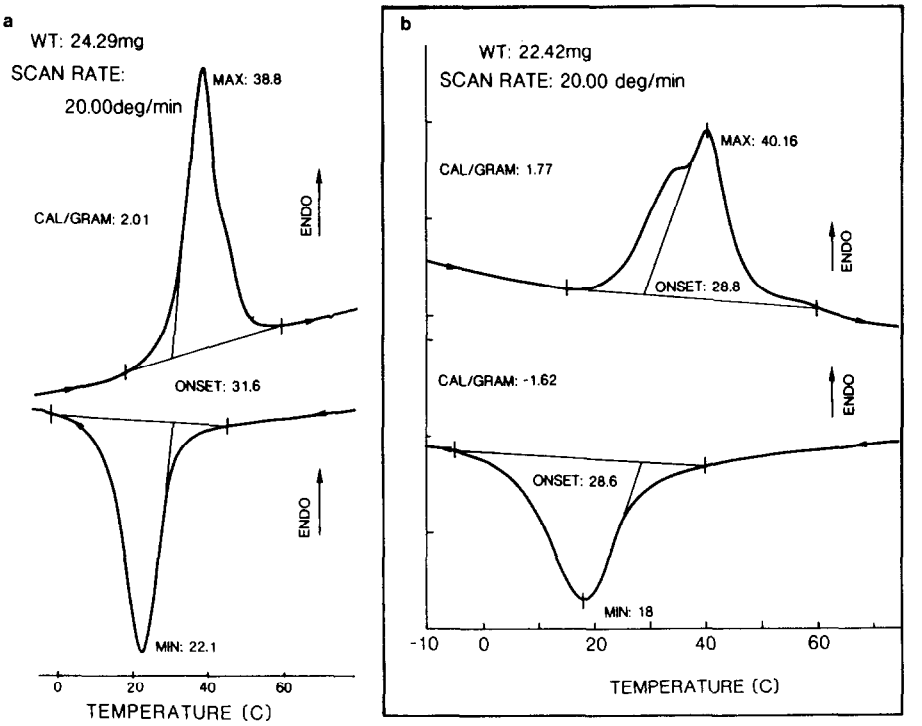

FIG. 3. Thermal characteristics of the phase transition with apparent hysteresis in the high-temperature phase of $LiZr_2(PO_4)_3$. (a) Sample heated for 6 hr at 1250°C. (b) Sample heated for 4 h at 1250°C and which has stayed a few days below room temperature.

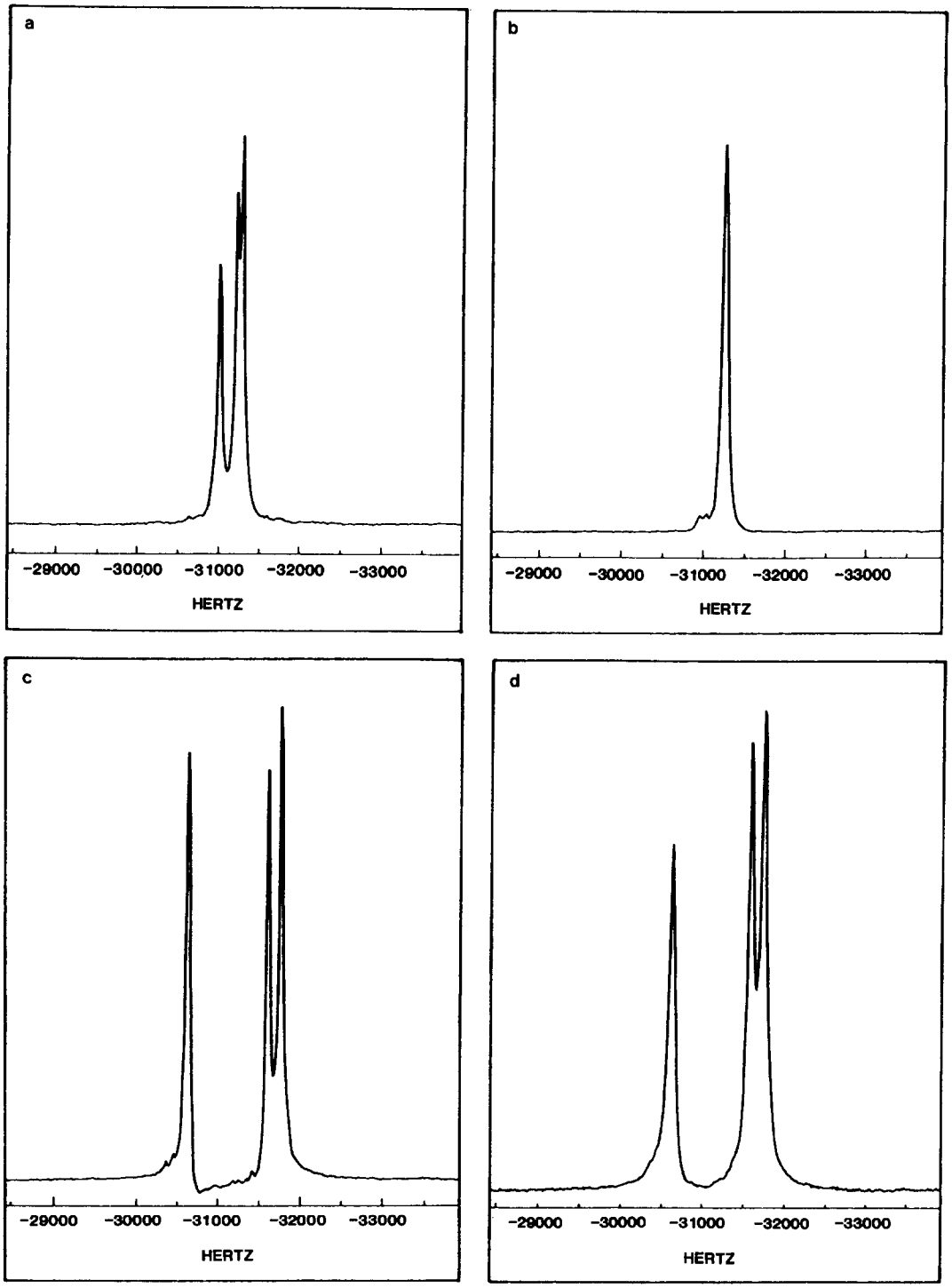

FIG. 4. ^{31}P MAS NMR spectra (145.8 MHz) for $LiZr_2(PO_4)_3$ samples. Sample fired at 1200°C with a pure high-temperature phase: (a) at 293 K, the three peaks correspond to three crystallographically distinct positions of the Cc space group for phosphorus atoms; (b) at 373 K, the peak corresponds to one P position of the $R\bar{3}c$ space group. Sample fired at 900°C with a pure low-temperature phase: (c) at 293 K and (d) at 373 K; the three peaks correspond to three crystallographically distinct positions of the $P2_1/n$ space group for phosphorus atoms. Sample fired at 1100°C with a mixture of phases: (e) at 293 K and (f) at 373 K.

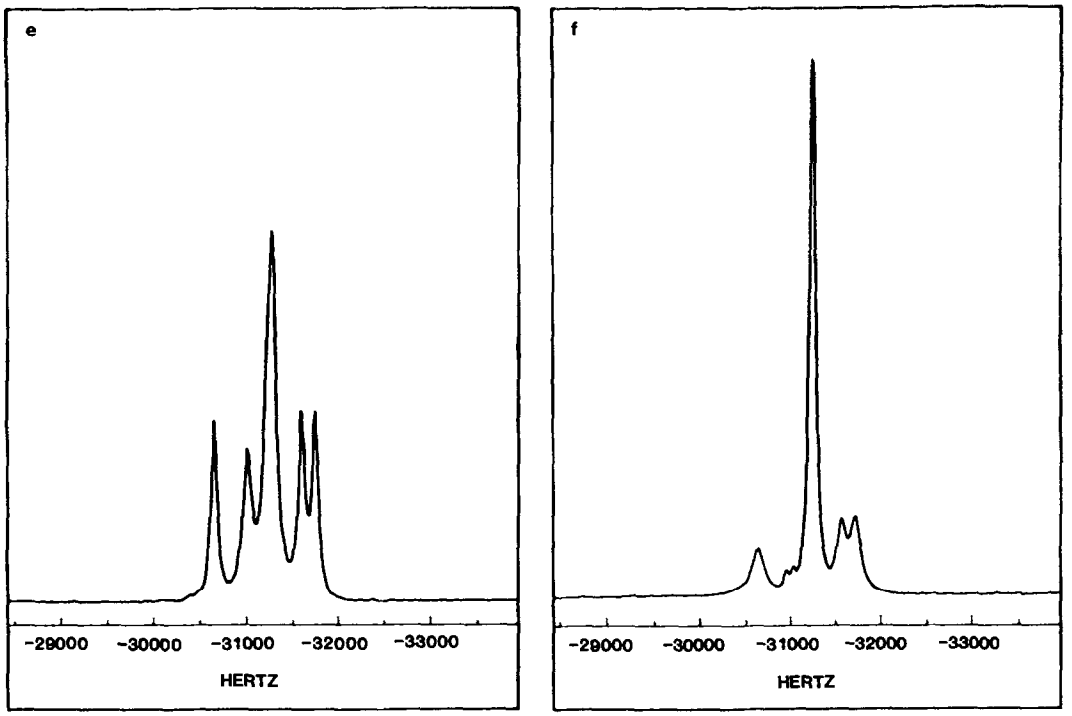

FIG. 4—*Continued*

space groups $C2/c$ and Cc. In the Cc group, phosphorus atoms occupy three positions (Fig. 4a) instead of only two as in the $C2/c$ group. Therefore, the NMR spectrum of the figure clearly indicates that the monoclinic NASICON-type phase belongs to the Cc space group. Nevertheless, some samples, which had been previously heated above the phase transition, exhibited only two peaks with an intensity ratio 1–2 corresponding to the occupation of the two positions (8*f* and 4*e*) of the $C2/c$ space group ($Z = 4$).

At 100°C, the ^{31}P MAS NMR spectra showed only one peak (Fig. 4b) consistent with the occupation by the phosphorus atoms of the 18*e* position of the rhombohedral $R\bar{3}c$ space group ($Z = 6$). Therefore, the phase transition is obviously associated with the monoclinic → rhombohedral transformation. Moreover, NMR and DSC data seem to indicate the following two structural transformations: $Cc \rightarrow C2/c \rightarrow R\bar{3}c$ during heating and $R\bar{3}c \rightarrow C2/c$ crossover only during cooling. The return of the sample to the Cc space group required a long period at low temperature to completely relax the skeleton.

Transport properties. The temperature dependence of the conductivity for $LiZr_2(PO_4)_3$ samples with a pure high-temperature phase is shown in Fig. 5a. The monoclinic → rhombohedral transition also leads to a slope discontinuity on the conducting curve. Plotting $\log \sigma T$ vs $1/T$ can be done with two half-straight lines whose slopes correspond to the activation energies, i.e., $E_a = 0.65$ eV for the lower temperature range ($t < 50$°C) and $E'_a = 0.42$ eV for the higher temperature range ($t > 50$°C). The ionic conductivity is 3.3×10^{-6} $(\Omega\ \text{cm})^{-1}$ at room temperature and 1.2×10^{-2} $(\Omega\ \text{cm})^{-1}$ at 300°C.

The ^{31}P NMR signals have been observed

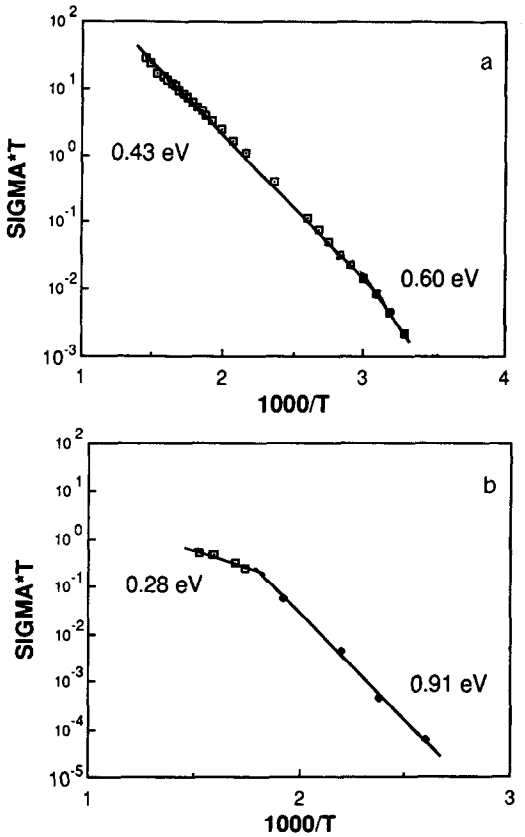

FIG. 5. σT (Ω^{-1} cm^{-1} K) versus inverse temperature (K^{-1}) for $LiZr_2(PO_4)_3$ samples. (a) Sample fired at 1200°C with a pure high-temperature phase; a slope discontinuity is observed around 40°C. (b) Sample fired at 900°C with a pure low-temperature phase; a slope discontinuity is observed around 300°C.

at 16.5 and 145.8 MHz. Between RT and 600°C, the ^{31}P free induction decays observed at 16.5 MHz follow approximately the law $M_0 \exp(-\Delta_p^2 t^2)$. Figure 6a shows the temperature dependence of the square root of the experimental second moment Δ_p^2 of the ^{31}P signal. Below the phase transition, a value of about Δ_p = 1000–1100 Hz is observed and at the transition, the ^{31}P linewidth suddenly decreases from 1050 to 800 Hz. Other experimental values of Δ_p can be obtained from the ^{31}P resonance lines at 145.8 MHz (Fig. 6b). Measurement of the half-widths δ_p at half intensity leads to the values of Δ_p = 1190 Hz at RT and Δ_p = 700 Hz at 373 K using the relation $\delta_p = \Delta_p \times [2\mathrm{Ln}(2)]^{1/2}$. This indicates that the ^{31}P linewidth is only slightly dependent on the frequency and that the line broadening is essentially due to dipolar interactions.

Moreover, the half-width δ_{Li} at half intensity of the central ^7Li signal at 140 MHz changes from 1130 Hz at RT to 450 Hz at 100°C (Fig. 6e). The corresponding values of Δ_{Li} are 960 Hz at RT and 380 Hz at 100°C.

At RT, using static second moment calculations in the rigid regime lattice (crystallographic data of Ref. (*9*)), Petit and Sapoval (*10*) have shown that the dipolar interactions give a ^{31}P line broadening of 1150 Hz with about 700 Hz due to the P–Li contribution and a ^7Li line broadening of 1000 Hz with about 700 Hz due to the Li–P contribution and of 200 Hz due to the Li–Li contribution. Therefore, our experimental line widths are compatible with that of a Gaussian line using the previous second moment calculations, and no lithium motion takes place before the transition.

At the phase transition, as noted by Petit and Sapoval (*10*), the sharp drop in linewidth of both ^7Li and ^{31}P, corresponding to the partial averaging of the dipolar interactions (Li–Li contribution and about 50% of the P–Li contribution), can be attributed to the onset of Li^+ motion after the phase transition, in agreement with the lower activation energy observed on the conductivity curve.

2. *Low-Temperature Phase*

Structure and phase transition. XRD patterns (Fig. 1) from $LiZr_2(PO_4)_3$ powders heated at 900°C show reflections which have been recently indexed by Casciola *et al.* (*11*) on the basis of a monoclinic cell with a = 15.299 Å, b = 8.940 Å, c = 8.816 Å, and β = 125.98°. The unit cell changes to orthorhombic around 300°C (a = 12.453 Å,

b = 8.954 Å, c = 8.859 Å, and V/Z = 247 Å^3), and a weak endothermic effect is associated with this phase transition.

In fact, the XRD pattern can be indexed on the basis of another monoclinic cell with the parameters a = 8.816 Å, b = 8.940 Å, c = 12.381 Å, β = 90.79°, and V/Z = 244 Å^3, which clearly displays the slight distortion of the orthorombic cell. The observed extinctions are consistent with the $P2_1/n$ space group. Moreover, this orthorombic-type structure has been previously observed in other lithium compounds such as $Li_3Fe_2(PO_4)_3$ (*13–15*), $Li_3Sc_2(PO_4)_3$ (*16*), and $Li_3In_2(PO_4)_3$ (*17*) and is isotypic with the monoclinic modification of $Fe_2(SO_4)_3$ (a = 11.665 Å, b = 8.558 Å, c = 8.310 Å, and β = 90.76°). This 3D skeleton structure (*18, 19*) is made of SO_4 tetrahedra sharing corners with FeO_6 octahedra. The O_2T_3 units are similar to those found in the NASICON-type structure but the arrangement of the units is different: there are alternating slabs with units oriented approximately along the [120] direction (slab I) and slabs with units oriented along the [1$\bar{2}$0] direction (slab II) (Fig. 2b). In lithium compounds, Li^+ ions have a tetrahedral coordination.

^{31}P MAS NMR spectra realized at 20 and 100°C confirm both the absence of a phase transition near 50°C and the different distribution of the phosphorus atoms in the monoclinic phase in comparison with that observed in the NASICON-type structure. For the two temperatures (Figs. 4c and 4d), three peaks are observed corresponding to three positions of the $P2_1/n$ space group. The frequency discrepancies between these peaks are much greater than those noted for NASICON-type structures, which probably indicates more distorted PO_4 tetrahedra in agreement with the higher transition temperature (only two peaks are expected for the orthorhombic phase, probably belonging to the *Pcan* space group (*14*)).

Transport properties. The temperature dependence of $LiZr_2(PO_4)_3$ samples with a pure low-temperature phase is shown in Fig. 5b. The monoclinic → orthorhombic transition also leads to a slope discontinuity on the conducting curve with two activation energies: E_a = 0.91 eV for the lower temperature range (t < 300°C) and E'_a = 0.28 eV for the higher temperature range (t > 300°C). In agreement with MAS NMR data, no anomaly is present in the range 25–60°C. The ionic conductivity is very low at room temperature and can be extrapolated to 10^{-10} $(\Omega\ cm)^{-1}$. Due to the high activation energy, the conductivity rises to about 5.10^{-4} $(\Omega\ cm)^{-1}$ at 300°C.

The ^{31}P NMR signals have been observed at 16.5 and 145.8 MHz. Between RT and 600°C, the ^{31}P free induction decays observed at 16.5 MHz follow approximately the law $M_0 \exp(-\Delta_p^2 t^2)$. Figure 6b shows the temperature dependence of the square root of the experimental second moment Δ_p^2 of the ^{31}P signal. At RT, a value of about Δ_p = 1050 Hz is observed, which progressively decreases to 750 Hz at 120°C. No significant change is observed at the phase transition (300°C). For the ^{31}P resonance line obtained at 145.8 MHz (Fig. 6d), the half widths δ_p at half intensity are 2400 Hz at RT and 2300 Hz at 100°C. This indicates that the ^{31}P linewidth is drastically dependent on the frequency and that the line broadening at 145.8 MHz is essentially due to the chemical shift contribution in agreement with the highly separated three peaks observed on the MAS spectra.

The half-width δ_{Li} at half intensity of the central ^{7}Li signal at 140 MHz changes from 1100 Hz at 293 K to 680 Hz at 373 K (Fig. 6f). Using the relation $\delta_{Li} = \Delta_{Li} \times [2Ln(2)]^{1/2}$, the corresponding values of Δ_{Li} are 930 Hz at RT and 580 Hz at 100°C.

For this structural type, there is no calculation for the rigid regime lattice because the crystal structure determination has not yet been performed. Nevertheless, one can suppose that the average distances between

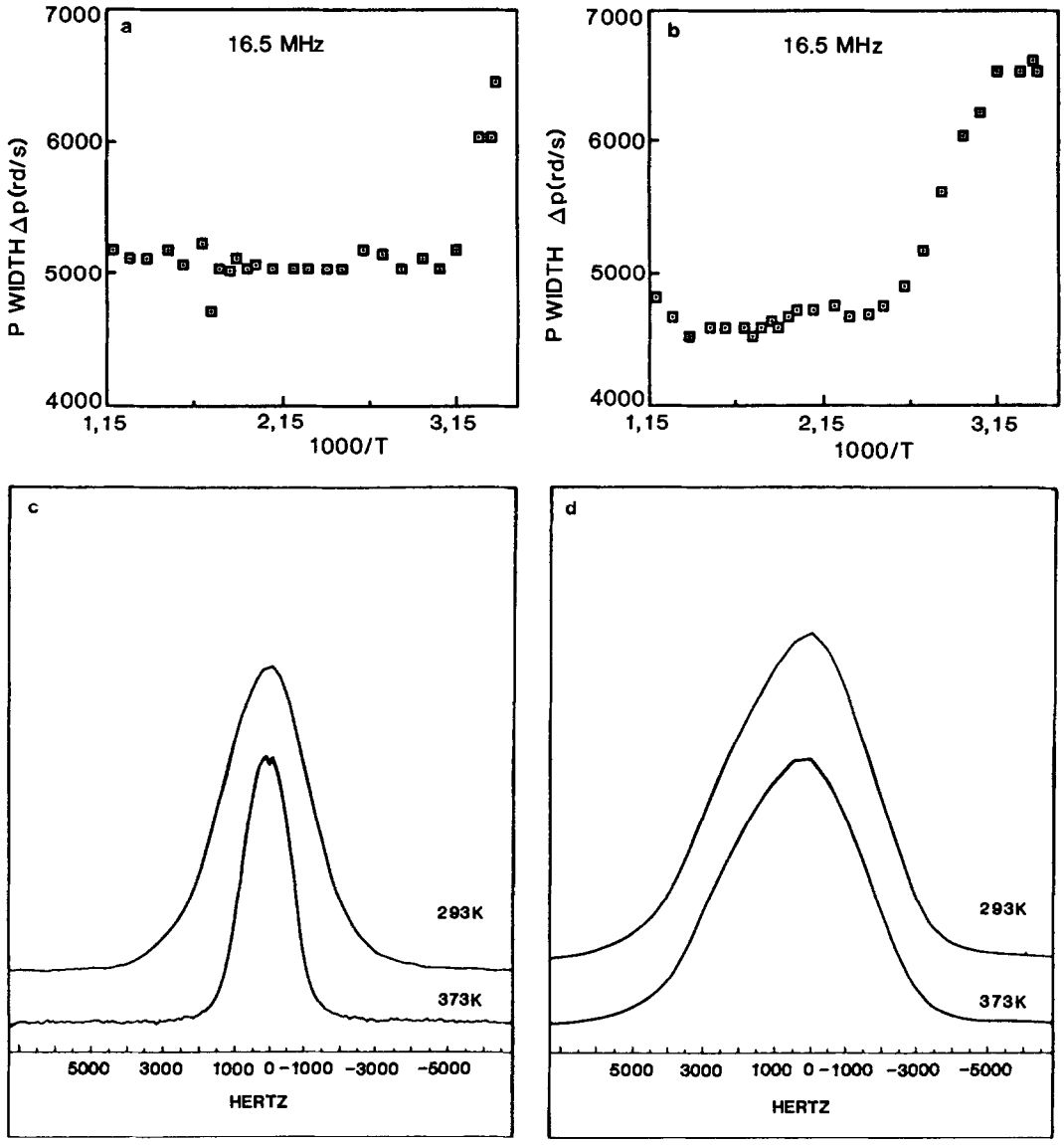

FIG. 6. Evolution of the NMR absorption spectra with temperature. ^{31}P at 16.5 MHz. (a) Variation of width Δ_P as a function of inverse temperature for the sample fired at 1200°C and (b) for the sample fired at 900°C. Δ_p stands for the square root of the experimental second moment obtained from the approximate Gaussian free induction decay $M_0 \exp(-\Delta_p^2 t^2/2)$. ^{31}P at 145.8 MHz. (c) Sample fired at 1200°C with a pure high-temperature phase. The half-width at half intensity is δ_p = 1400 Hz at 293 K and 800 Hz at 373 K. (d) Sample fired at 900°C with a pure low-temperature phase. The half-width at half intensity is δ_p = 2400 Hz at 293 K and 2300 Hz at 373 K. ^7Li at 140 MHz. (e) Sample fired at 1200°C with a pure high-temperature phase. The half-width at half intensity of the central line is δ_{Li} = 1130 Hz at 293 K and 450 Hz at 373 K. (f) Sample fired at 900°C with a pure low-temperature phase. The linewidth at half intensity of the central line is δ_{Li} = 1100 Hz at 293 K and 680 Hz at 373 K.

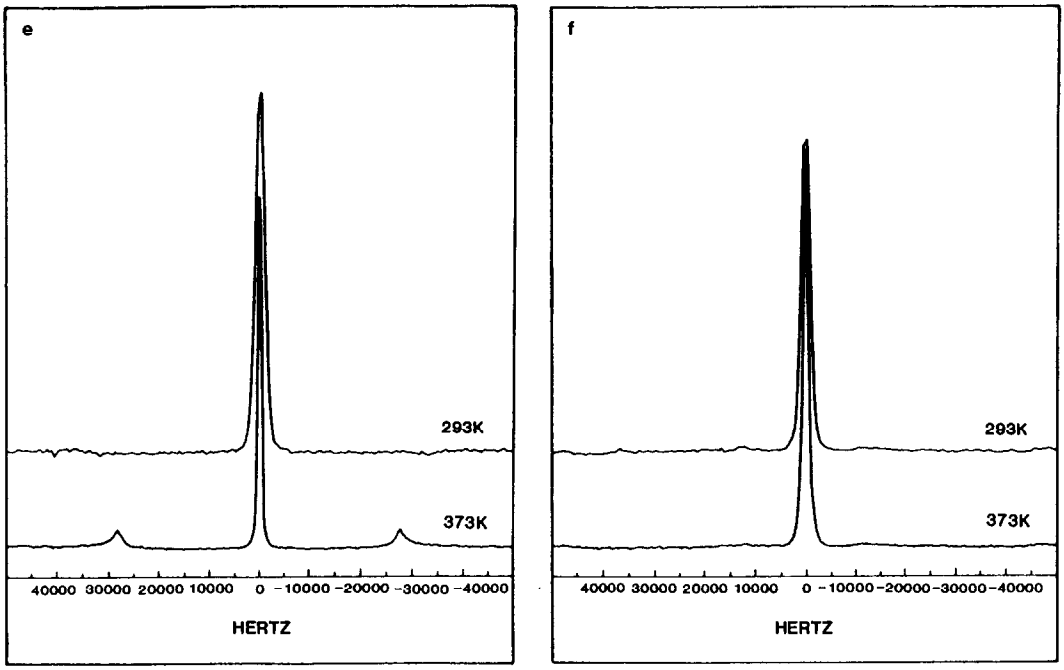

FIG. 6—*Continued*

atoms are very close to those observed in the NASICON-type structure. Consequently, at RT, the values of $\Delta_{Li} = 930$ Hz at 140 MHz and of $\Delta_P = 1050$ Hz at 16.5 MHz indicate a nearly rigid regime with no lithium motion.

In the temperature range from RT to 120°C, the continuous decrease in linewidth of both ^7Li at 140 MHz and ^{31}P at 16.5 MHz, corresponding to the partial averaging of the dipolar interactions, can be due to the progressive onset of a Li^+ local motion in agreement with the high activation energy before the phase transition. Further work, such as measurements of relaxation time, is required to characterize the lithium diffusion mechanism after the phase transition.

3. *Diphasic Samples*

Structure and phase transitions. XRD patterns (Fig. 1) from $LiZr_2(PO_4)_3$ powders heated between 900 and 1200°C generally exhibit both reflections of the low-temperature phase and reflections of the high-temperature phase. Relative intensity of the X-ray peaks corresponding to the low-temperature phase normally decreases when the firing time increases from 3 to 6 hr and especially when the firing temperature increases from 900 to 1200°C. It is clear that the low-temperature → high-temperature phase transformation takes place over a large temperature range because it requires the breaking and formation of numerous chemical bonds.

The monoclinic–rhombohedral transition of the high-temperature phase is always observed on the DSC curves from diphasic samples, with a slight shift toward the high temperature (onset at 50–55°C) and with a continuous increase in the intensity with increasing firing temperature. In contrast, only a very weak thermal effect (0.2 cal. g^{-1}) due to the monoclinic–orthorhombic transformation of the low-temperature

phase has been seen for the powder heated at 1100°C for 4 hr.

^{31}P NMR spectra at room temperature (Fig. 4e) present five peaks corresponding to the coexistence of the three positions of the $P2_1/n$ space group for the LT phase and to the coexistence of the two positions of the $C2/c$ space group for the HT phase. Therefore, at the local scale, the sample does not contain a significant concentration of PO_4 groups with intermediary distortions between those observed for the HT and LT phases. ^{31}P NMR spectra at 100°C (Fig. 4f) show four peaks corresponding to the addition of the three positions of the $P2_1/n$ space group for the LT phase and to the addition of only one position of the $R\bar{3}c$ space group for the HT phase. This indicates that the presence of the LT phase does not drastically influence the monoclinic → rhombohedral transition of the HT phase.

Transport properties. Conductivity measurements have been performed for different $LiZr_2(PO_4)_3$ samples heated between 900 and 1200°C. For each sample, the LT/HT phase ratio has been deduced from the ratio between the sum of the NMR peak areas corresponding to each phase. For example, a ratio of 0.45 has been obtained from the spectrum represented in Fig. 4e. Figure 7 shows the temperature dependence of the electrical conductivity for different phase ratios. It should be noted that in the temperature range 50–300°C, when the phase ratio changes from 1 to 0, the activation energy gradually decreases from 0.91 eV, the value corresponding to the pure LT phase, to 0.42 eV, the value previously obtained for the pure HT phase.

The ^{31}P NMR signals have been observed at 16.5 MHz for the sample fired at 1100°C with a phase ratio of 0.45. Figure 8 shows the temperature dependence of the square root of the experimental second moment Δ_p^2 of the ^{31}P signal. The sample clearly exhibits an intermediate behavior between those shown by HT and LT phases.

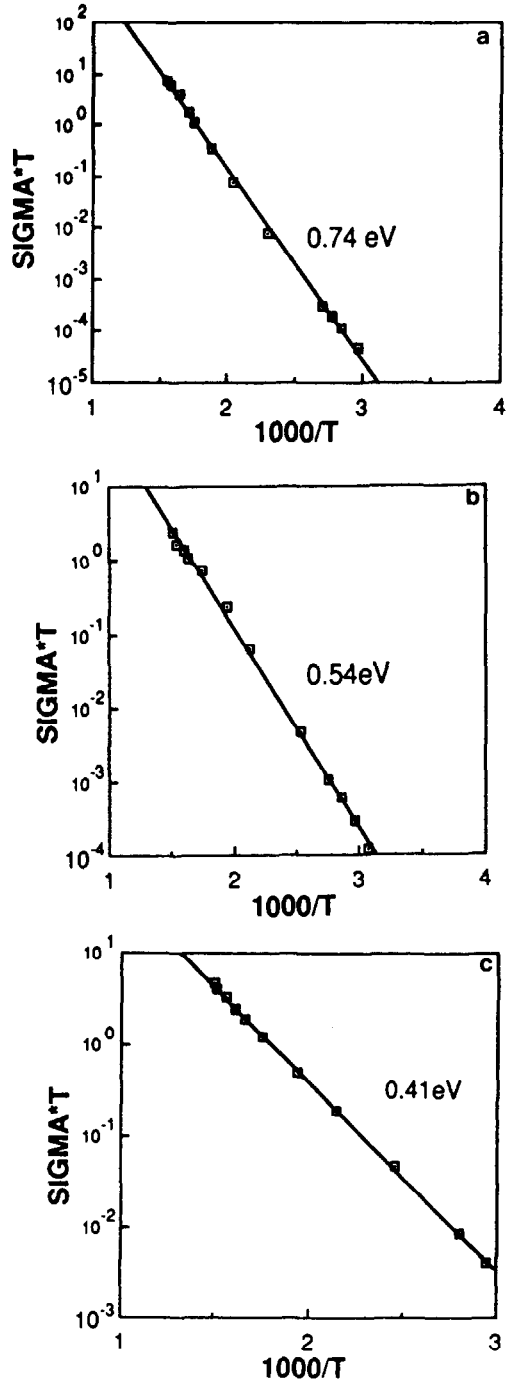

FIG. 7. Electrical characteristics for diphasic $LiZr_2(PO_4)_3$ samples with (a) 46%, (b) 10%, and (c) 0% of low-temperature phase. For 100% the activation energy is 0.91 eV.

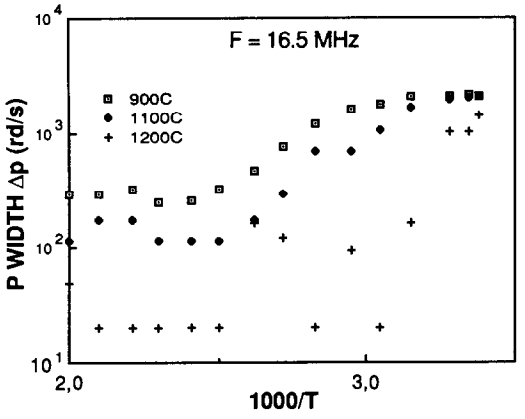

FIG. 8. Temperature dependence of ^{31}P width Δ_p at 16.5 MHz as a function of inverse temperature for samples fired at different temperatures.

Conclusion

We have demonstrated two different phases for $LiZr_2(PO_4)_3$ materials prepared by sol/gel technique:

—a high-temperature phase, prepared at 1200°C, which exhibits a NASICON-type structure and a monoclinic (generally *Cc* space group) → rhombohedral ($R\bar{3}c$) transformation at about 40°C. This first order transition is associated with a slope discontinuity on the conducting curve (change in the activation energy from 0.65 to 0.42 eV) and with a narrowing of the ^7Li and ^{31}P NMR lines due to the sharp appearance of a lithium motion. This leads to high conducting properties above the phase transition $\sigma = 1.2.10^{-2}$ $(\Omega\ cm)^{-1}$ at 300°C. In the monoclinic NASICON-like phase, the high polarizing Li^+ ions are not mobile and must therefore be strongly bonded to the lattice. Further X-ray structural investigations on single crystals are necessary to localize lithium ions in the structure.

—a low temperature phase, prepared at 900°C, which exhibits the β-$Fe_2(SO_4)_3$-type structure and a monoclinic ($P2_1/n$ space group) → orthorhombic (probably *Pcan*) transformation at 300°C. This structure differs from the NASICON-type structure by the arrangement of the $(ZrO_6)_2(PO_4)_3$ units. The transition is also associated with a slope discontinuity on the conducting curve (change in the activation energy from 0.91 to 0.28 eV). A local lithium motion progressively takes place between RT and 120°C and the high activation energy, below the transition, leads to the crossover from a poorly conducting state at RT ($\sigma = 10^{-10}$ $(\Omega\ cm)^{-1}$) to a conducting state at 300°C ($\sigma = 5.10^{-4}$ $(\Omega\ cm)^{-1}$).

The LT/HT phase ratio in diphasic samples, prepared between 900 and 1200°C, has been deduced from MAS NMR peak intensities. As expected, the phase ratio is reduced when the firing temperature of the sample increases. A surprising fact is that both resistivity and activation energy progressively increase with the phase ratio. Then, for a diphasic sample, the electrical properties are intermediate between that of the HT phase and that of the LT phase. These results explain the confused previous observations on $LiZr_2(PO_4)_3$ materials and can be attributed to the presence of some local defects in the higher conducting part of the sample (HT phase) which could be the memory of the LT → HT phase transformation. The concentration of these defects becomes very weak at a high firing temperature. However, other explanations, such as microstructure or surface effects, could probably be advanced.

References

1. H. Y.-P. HONG, *Mater. Res. Bull.* **11**, 173 (1976).
2. J. P. BOILOT, G. COLLIN, AND PH. COLOMBAN, *in* "Progress in Solid Electrolytes" (T. Wheat, A. Ahmad, and A. Kuriakose, Eds.), p. 94, Energy, Mines, Resources, Ottawa, Canada (1983).
3. M. SLJUKIC, B. MATKOVIC, B. PRODIC, AND S. SCAVINCAR, *Croat. Chem. Acta Zagreb.* **39**, 145 (1967).
4. B. E. TAYLOR, A. D. ENGLISH, AND T. BERZINS, *Mater. Res. Bull.* **12**, 171 (1977).

5. M. A. SUBRAMAMIAN, R. SUBRAMAMIAN, AND A. CLEARFIELD, *Solid State Ionics* **18/19,** 562 (1986).
6. J. P. BOILOT AND PH. COLOMBAN, *in* "Sol Gel Technology for Thin Films, Fibers, Preforms, Electronics and Specialty Shapes" (L. C. Klein, Ed.), p. 303, Noyes Press, Park Ridge, NJ (1988).
7. H. PERTHUIS AND PH. COLOMBAN, *Mater. Res. Bull.* **19,** 621 (1984).
8. M. BARJ, H. PERTHUIS, AND PH. COLOMBAN, *Solid State Ionics* **9/10,** 845 (1983).
9. D. PETIT, PH. COLOMBAN, G. COLLIN, AND J. P. BOILOT, *Mater. Res. Bull.* **21,** 365 (1986).
10. D. PETIT AND B. SAPOVAL, *Solid State Ionics* **21,** 293 (1986).
11. M. CASCIOLA, U. COSTANTINO, L. MERLINI, I. G. KROGH ANDERSEN, AND E. KROGH ANDERSEN, *Solid State Ionics* **26,** 229 (1988).
12. U. VON ALPEN, M. F. BELL, AND W. WICKELHAUS, *Mater. Res. Bull.* **14,** 1317 (1979).
13. F. D'YVOIRE, M. PINTARD-SCREPEL, E. BRETEY, AND M. DE LA ROCHERE, *Solid State Ionics* **9/10,** 851 (1983).
14. I. A. VERIN, E. A. GENKINA, AND B. A. MASKIMOV, *Sov. Phys. Crystallogr. (Engl. Transl.)* **30,** 394 (1985).
15. B. A. MASKIMOV, L. A. MURADYAN, E. A. GENKINA, AND V. I. SIMONOV, *Sov. Phys. Dokl. (Engl. Transl.)* **31,** 370 (1986).
16. I. P. KONDRATYUK, B. A. MASKIMOV, AND L. A. MURADYAN, *Sov. Phys. Dokl. (Engl. Transl.)* **32,** 95 (1987).
17. D. TRAN QUI AND S. HAMDOUNE, *Acta Crystallogr. C* **43,** 397 (1987).
18. P. B. MOORE AND T. ARAKI, *N. Jb. Miner. Abh.* **121,** 208 (1974).
19. P. C. CHRISTIDIS AND P. J. RENTZEPERIS, *Z. Kristallogr.* **141,** 233(1975).